Materials Science in Semiconductor Processing 59 (2017) 29–34

Contents lists available at ScienceDirect

Materials Science in Semiconductor Processing

journal homepage: www.elsevier.com/locate/mssp

Improving the performance of solar cells with novel buffer structure by the chemical bath deposition technique

Jia-Show Ho[a,b], Shih-Cheng Chang[a], Jyh-Jier Ho[a,*], Wei-Tse Hsu[c], Chien-Chih Chiang[c], Song-Yeu Tsai[c], Sheng-Shih Wang[a], Cheng-Kai Lin[d], Chau-Chang Chou[a], Chi-Hsiao Yeh[d], Kang L. Wang[b]

[a] Department of Electrical Engineering, National Taiwan Ocean University, No. 2, Peining Rd., Keelung 20224, Taiwan
[b] Department of Electrical Engineering, University of California, Los Angeles, CA 90095, USA
[c] Lab. of Green Energy & Environment Research, Industrial Tech Research Institute, Hsinchu1, Taiwan
[d] Department of Surgery, Chang Gung Memorial Hospital, Keelung 20400, Taiwan

ARTICLE INFO

Keywords:
Cu(ln,Ga)Se_2 (CIGS) solar cells
Chemical bath deposition (CBD)
ZnS/CdS-buffer
Anti-reflective effect
Commercial PV applications

ABSTRACT

This paper explores and compares the characteristics of eight different kinds of Cu(In, Ga)Se_2 (CIGS) solar cells. Through the technique of chemical bath deposition (CBD), single- (i-ZnO) and double-layer (ZnS/CdS) CIGS cells were prepared and evaluated. The results of this research signify the potential of high-performance CIGS cells for photovoltaic (PV) industrial applications. This study focused on the growth-dependency and optical properties of ZnS/CdS-buffer stacked thin films, which were prepared through the CBD process. The best sample developed from this process consisted of a double-layer buffer and no i-ZnO layer. This sample yielded a conversion efficiency (η) of 9.23% and a short-circuit current density (J_{SC}) of 26.72 mA/cm^2. The performance of this sample was about 25% (absolute gain) better than that of the standard CdS cells.

Furthermore, the average quantum efficiency in the short wavelength range (350–500 nm) for two of the ZnS/CdS buffer structures was 6.8% better than that of a single-layer CdS cell. This improvement can be attributed to the anti-reflective effect of the ZnS/CdS buffer structure, which increases ~~the~~ light-intensity incident on the main absorption layer. In addition, the ZnS/CdS-buffer layer not only eliminates the need for an i-ZnO layer but also reduces the usage of toxic Cd. The procedures to develop these flexible CIGS cells containing a ZnS/CdS buffer structure are simple, efficient, and reliable. These eco-friendly cells could be effectively applied to mass production for commercial PV applications.

1. Introduction

Photovoltaic (PV) technology utilizes one of the most attractive energy sources on the planet—sunlight. Perhaps the greatest drawbacks of solar cells include high production cost and low durability. Overcoming these two shortcomings can greatly enhance the competitiveness of photovoltaic devices and promote the use of renewable energy. Amongst thin-film PV cells, chalcopyrite solar cells consisting of a copper-indium-gallium-selenide (Cu(In,Ga)Se_2, CIGS) absorber have shown promise owing to their superior power-conversion efficiency [1].

In thin-film solar cells with a CIGS absorber, cadmium sulfide (CdS) is generally introduced as a buffer layer to achieve high overall efficiencies. However, CdS has a band gap of only ~2.45 eV, which limits cell performance as its low transparency in the short-wavelength spectrum leads to photocurrent loss [2]. Zinc sulfide (ZnS), an n-type II–VI semiconductor with a wider direct band gap of 3.5–3.8 eV at room temperature [2–4], could be a better material for UV-sensitive buffering layers and coating films in solar cells. Due to its wide bandgap, ZnS can not only enhance the short-wavelength response of PV solar cells but also allow more high-energy photons to penetrate the buffer and reach the junction between the window and the absorber, thus improving cell performance.

Moreover, toxicity hazards from the production and use of the CdS layer further justify the investigation of ZnS as an alternative buffer layer for PV devices [4,5]. Zn-based thin films deposited by chemical-bath-deposition (CBD) process (with non-vacuum deposition) have already been established as alternative buffer materials for PV devices, and a module efficiency of 18.6% has been achieved with the corresponding CIGS-based solar cells [2,6]. Thus in this work, we

* Corresponding author.
E-mail address: jackho@mail.ntou.edu.tw (J.-J. Ho).

http://dx.doi.org/10.1016/j.mssp.2016.09.044
Received 10 October 2015; Received in revised form 16 September 2016; Accepted 30 September 2016

deposited ZnS thin films using the CBD technique. Thiourea was used as the source of sulphur, $ZnCl_2$ as the source of Zn, and NH_3 as a complexing agent for the Zn-salt precursor. The structural and optical properties of the films measured at each step of cell process were carefully studied and compared.

In the design of CIGS thin-film solar cells on flexible substrates, we focused on the development of double-layered buffers (ZnS/CdS), a novel structure, with high transmittance in the short-wavelength region, in the meantime maintaining good interface characteristics between the buffer layer and the CIGS absorber on the tuneable band-gap effect. ZnS thin film was deposited on the CdS surface through the CBD process to form a stack of buffer layers, denoted as ZnS/CdS. The structural and optical features of the thin films fabricated by CBD were then analyzed and compared.

Two main objectives of this experiment were to improve the quantum efficiency (QE) in the short-wavelength region and to increase photocurrent and power-conversion efficiency (η) of CIGS solar cells. In addition to these two goals, we also explored the idea of using i-ZnO layer as an alternative to the ZnS/CdS double-layer buffer in CIGS solar cells. Lastly, in order to promote future commercialization of these techniques, we shortened chemical reaction time, reduced process steps, and lowered production cost.

2. Experiments and measurements

Fig. 1 shows the flow chart for the fabrication of the proposed flexible CIGS-based solar cells (stainless-steel substrates) under various conditions. This process allowed for the evaluation of the performance of CIGS thin-film solar cells with ZnS/CdS buffer. The initial solutions to develop CBD-CdS films were prepared from anhydrous cadmium chloride (0.12 M $CdCl_2$ as the Cd^{2+} source), thiourea (0.3 M $CS(NH_2)_2$ as the S^{2-} source), ammonia (10 M NH_3 as the complexing agent), ammonium chloride (NH_4Cl). The CdS thin film was grown on the CIGS absorber layer at a temperature of 65 °C for 5 min. In addition, ZnS thin film was also prepared from an acidic solution containing $ZnSO_4$ [7] as a source of zinc, thiocarbamide ($SC(NH_2)_2$) [8] as a source of sulphur, and tartaric acid ($C_4H_6O_6$) [9] as the complexing agent. The acidic solution was prepared using

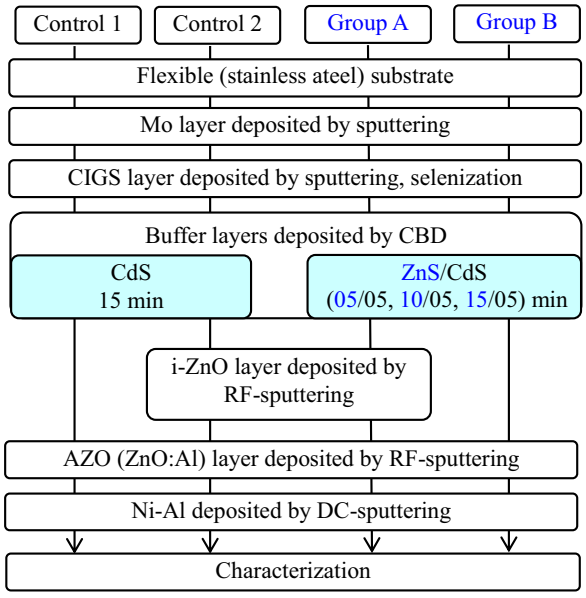

Fig. 1. The flow chart of CIGS solar cells fabricated by different processes and with different deposition times. Cells with and without an i-ZnO layer deposited by RF-sputtering were used for comparison. Double-layer ZnS/CdS films were deposited for 05/05, 10/05, 15/05 min, where the CdS film was deposited first on CIGS for 5 min then the ZnS was deposited on top of the CdS surface for different times (either 5 or 10 or 15 min). Inside this figure, the AZO means ZnO:Al.

Table 1
The CBD deposition times of the ZnS film were varied while keeping that of CdS constant at 5 min. Furthermore, a structure with an i-ZnO layer deposited by RF-sputtering was used (marked with Yes) for comparison among four kinds of samples, that is, Control 1, Control 2, group A, and group B.

Cell Samples	Buffers structures and CBD duration	ZnO layer included?
Control 1	CdS, 15 min	–
Control 2	CdS, 15 min	Yes
A1	ZnS/CdS, 05/05 min	Yes
A2	ZnS/CdS, 10/05 min	Yes
A3	ZnS/CdS, 15/05 min	Yes
B1	ZnS/CdS, 05/05 min	–
B2	ZnS/CdS, 10/05 min	–
B3	ZnS/CdS, 15/05 min	–

100 mL of $ZnSO_4$, 700 mL of $SC(NH_2)_2$ and 50 mL of $C_4H_6O_6$. The different solutions were prepared by adding the complexing agent $C_4H_6O_6$ with varying 0.001–0.05 M concentrations. In order to determine the optimal uniformity and penetrating features for the ZnS thin films, we measured the performance of ZnS at a constant temperature of 85 °C under three deposition times: 5, 10, and 15 min. Lastly, the final stage of this experiment involved analyzing the effects of RF-sputtering deposition of an i-ZnO layer on the cells. The CIGS-based solar cell area of our samples was 2×2 cm^2.

Table 1 lists the structures of the nano-scale buffer layer for four different samples: control 1, control 2, group A, and group B. In particular, group A and B contained three sub-samples. These sub-samples all had CdS deposited at 65 °C for 5 min and ZnS deposited at 85 °C; they differ by their ZnS deposition times, which were 5, 10, and 15 min. In addition, cells without an i-ZnO layer (Control 1 and group B) are marked as '-', and those with an i-ZnO layer (Control 2 and group A) are marked as 'Yes'; comparisons were then made between the two groups.

As shown in Table 2 deposited for different CBD processing times, the surface compositions (atomic ratios) of ZnS/CdS double-layer buffers were measured by the energy dispersive spectroscopy (EDS). Meanwhile, the optical and electrical properties of our cells were also measured using commercially available systems: scanning electron microscopy (Model: JSM-6500F), microwave-induced photo-conductance decay (μ-PCD) system (Model: U-2001), photovoltaic conversion efficiency measuring system (Model: Oriel-91192/ AM 1.5 GMM), and QE measurements (Model: C-995).

3. Results and discussion

To investigate the characteristics for the four samples with different buffer layers, we recorded scanning electron microscopy (SEM) images

Table 2
The surface composition and the corresponding images of EDS spectrum of ZnS/CdS double-layer buffers, deposited for different times.

Atomic	Atomic Ratio, %			
	CdS+ZnS (05+05)	CdS+ZnS (05 +10)	CdS+ZnS (05 +15)	CdS (15)
Cu K	17.43	17.47	16.80	16.42
In L	13.38	13.17	13.23	13.69
Ga K	9.47	7.30	9.70	4.68
Se K	42.85	44.43	43.59	37.17
Zn K	0.50	0.94	0.51	0
Cd K	3.12	2.87	2.48	7.24
S K	3.70	3.34	3.09	8.43
O K	9.58	10.48	10.60	12.37
Zn/(S+O)	0.04	0.07	0.04	0
Cd/(S+O)	0.23	0.21	0.18	0.35
S/(S+O)	0.28	0.24	0.23	0.41

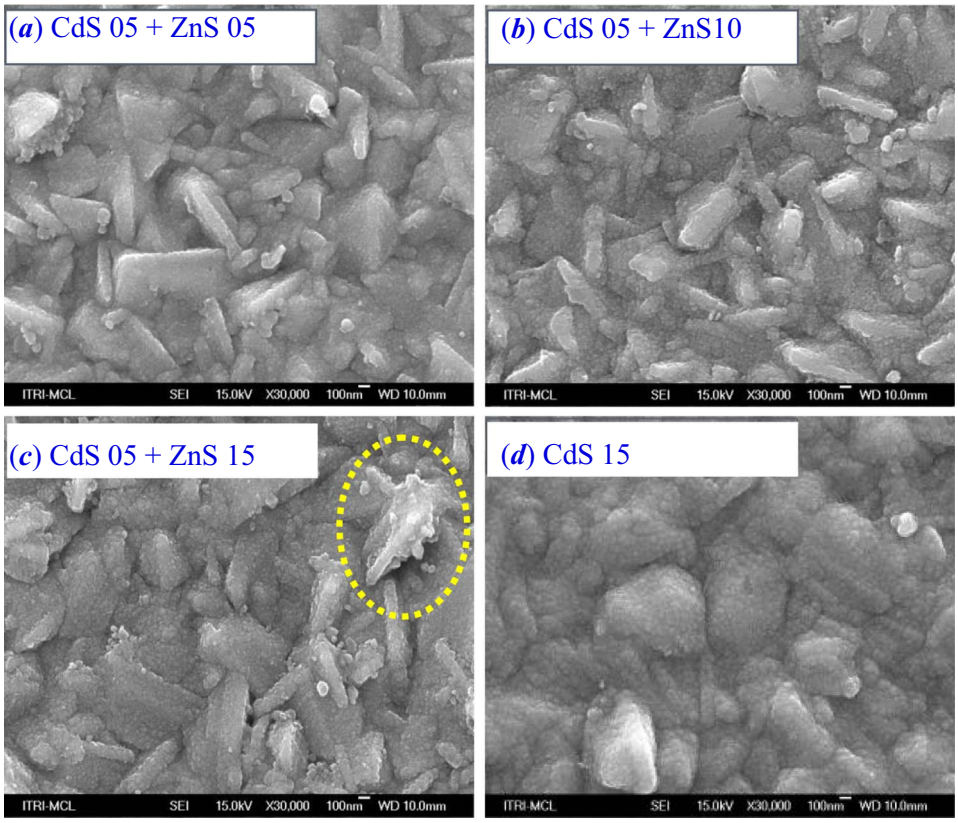

Fig. 2. Top-view SEM images of the buffer layer of CIGS solar cells, grown by CBD for different growth times; ZnS/CdS films grown for (*a*) 5/5 min, (*b*) 10/5 min, (*c*) 15/5 min, where CdS is first deposited on CIGS for 5 min then ZnS is deposited on top of the CdS surface. (*d*) CdS film grown for 15 min as a control reference.

of their respective buffers. Fig. 2(a)-(c) depicts the top-view surface morphologies of the ZnS/CdS double-layer buffer for these samples. The ZnS portion was grown at different deposition times while the CdS film was grown at the constant duration of 5 min. Fig. 2(d) shows the single-layer buffer (CdS grown for 15 min), which was used as a reference (denoted as Control 1).

Fig. 2 shows plan-view SEM images of CIGS devices coated with double-layers of ZnS/CdS (2a-c, samples B1-3) and with a single layer of CdS. In all cases, the surface morphology is dominated by the underlying granular structure of the CIGS which remains visible beneath the over-layers. For images a-c, (*i.e.* for samples with 5 min of CdS followed by 5,10 and 15 min of ZnS) the ZnS deposition makes the surface rough on a smaller scale than the CIGS grains, and at 15 mins (2c) nodules - presumably from homogeneous nucleation of the ZnS [10] start to appear. For the single layer of thick CdS (2d), the roughening of the deposit is similar but more pronounced.

Fig. 3(a)–(d) show the cross-section images of the buffer layer of CIGS solar cells in a one-to-one correspondence with Fig. 2(a)–(d). These images show that both ZnS and ZnS/CdS are double-layered structures, which cause them to appear more dense and uniform. These micrographs show that the double-layer buffer films have good adherence to the CIGS substrates without pinholes or cracks. We evaluated the variations in the film thickness, in the range 31–66 nm, as related to the CBD deposition time. These films exhibit tightly connected grain structures with good adhesion to the CIGS. Obviously for the ZnS/CdS double-layer buffer, the longer time of the deposited film increased its film thickness. As seen in the film cross-sections shown in Fig. 3(a)–(d), buffer layer structures of ZnS/CdS and CdS have different film growth rate, and the relationship between ZnS/CdS film thickness and deposition time of ZnS is not linear. It is comparatively easy to form a thin ZnS film with uniform thickness and excellent adhesion to the substrate via CBD [10].

Fig. 4(a) demonstrates the optical transmittance spectra for the ZnS/CdS and CdS buffer layers in the wavelength range 300–1100 nm. As deposition time increased, the film transmittance decreased, which lowered cell performance. It can be seen that the ZnS/CdS thin film has higher optical transmittance (~100%) than a conventional thick CdS layer (73.9%) at 520 nm. The average values of transmittance (T_{ave}) in visible-light range (400–700 nm) were calculated by the arithmetic mean, which is the sum of transmitting values as divided by its numbers. Therefore, the T_{ave}, values of transmittance (in %) and corresponding thickness (in nm) for the four different cell samples are listed in Fig. 4(b). The experiment showed that for the CdS deposition that was carried out at 65 °C for 60 min, the transmittance (76.6% average for Control 1 sample) did not meet the requirement value of at least 80% in the visible and infrared range [11]. However, as concluded in [5], this approach still led to a mutual characteristic improvement on optical transmittance of the ZnS/CdS film. The results show that ZnS has a high-energy band gap of 3.25 eV (more than 2.4 eV of CdS) in cubic forms, which yields a high transmittance in the visible range [12].

As seen in Fig. 4(b), both ZnS and CdS deposition times were 5 min for sample B1, and its light transmittance value was 96.9%, which was higher than those of B2, B3, and Control 1. For sample B2, the ZnS deposition time of the double-layer structure was 10 min, and the average transmittance dropped to 95.7%. This transmittance value was still much better than the 76.6% transmittance from Control 1. When the ZnS deposition time of the double-layer structure of sample B3 was increased to 15 min, the transmittance became 93.9%. The trend of the variation was consistent with the one illustrated by Shin et al. [13].

When the film thickness was kept constant, the transmittance values of double-layer buffers (B1, B2 and B3) at short wavelengths were far higher than that of conventionally processed CdS (Control 1). Compared to the ZnS/CdS double-layer structure, the top-down structure sequence of CIGS solar cell thin film was closely related to the energy gap value. A performance gain was achieved by alloying the

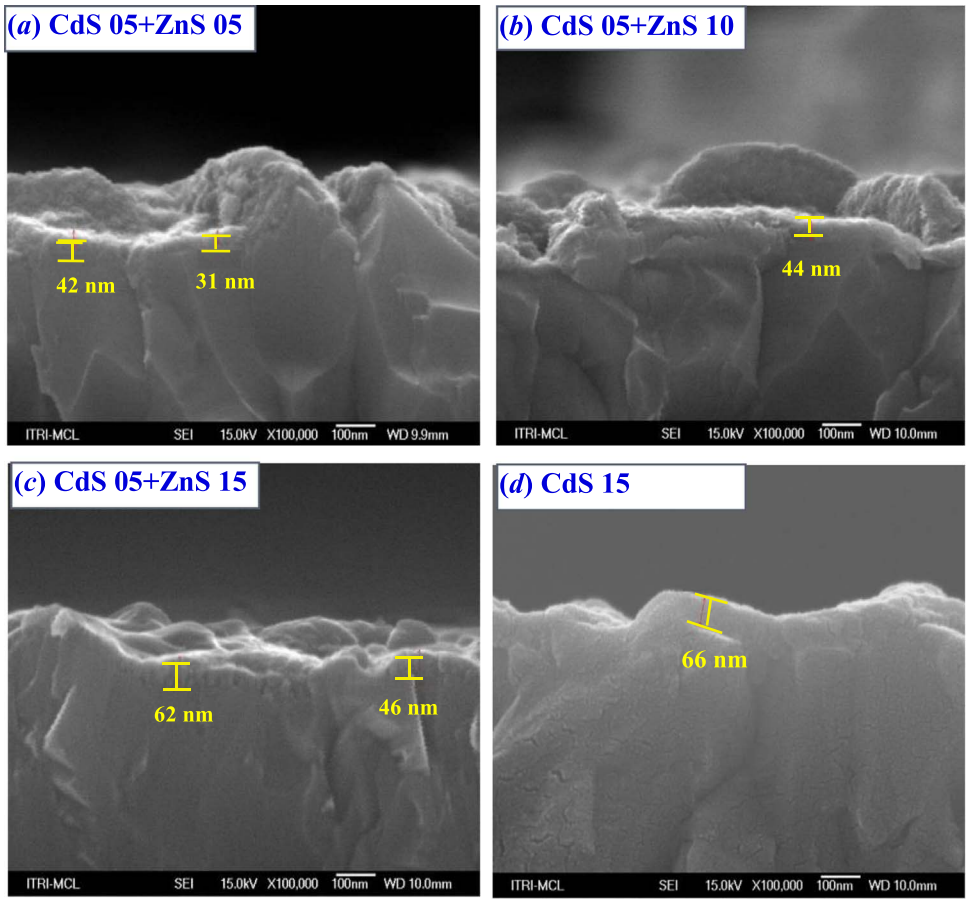

Fig. 3. SEM images of cross-section of the buffer layer of CIGS solar cells grown at different times; ZnS/CdS films grown for (*a*) 5/5 min, (*b*) 10/5 min, (*c*) 15/5 min, and CdS film for (*d*) 15 min Fig. 3(a–d) has a one-to-one correspondence to Fig. 2(a–d). The smaller characters, numerals and line segment inside photos indicating thickness in yellow. (For interpretation of the references to color in this figure legend, the reader is referred to the web version of this article.).

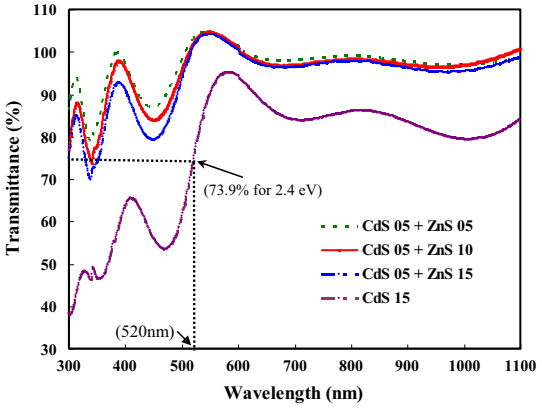

(*a*)

Cell Samples No.	Thickness (nm)	Transmittance (%)
B1, CdS (05) + ZnS (05)	31.0-42.2	96.9%
B2, CdS (05) + ZnS (10)	44.1	95.7%
B3, CdS (05) + ZnS (15)	45.6-61.9	93.9%
Ref 1, CdS15	66.0	76.6%

(*b*)

Fig. 4. (a): The optical transmittance of ZnS/CdS and CdS buffer layers as a function of the wavelength in the range (300–1100 nm) for different deposition times, observed on ITO. (b) The corresponding average values of visible light (400–700 nm) transmittance for the ZnS/CdS double-layer buffer and the CdS buffer for different deposition times.

CdS with ZnS to widen the band gap [14]. Since no apparent defects (e.g. pinholes) exist in the interfacial regions as seen in Fig. 3, the grown thin film structure could lead to an improvement of transmittance in the ZnS thin films [10]. The transmittance values for samples B1, B2, and B3 reveal that larger ZnS grains deposited on the surface of sample B3 (see Fig. 2(c)) will introduce scattering effects, which reduce optical transmittance [10]. As the deposition time of ZnS increased, the ZnS film became denser and the transmittance worsened.

All the thin films of the developed prototypes were analyzed by EDS using a JSM-6500F scanning electron microscope (SEM) equipped with a JEOL energy dispersive X-ray analyzer (shown in Table 2). When the ZnS buffer layer deposition time was 5 min, the atomic ratios for all the atoms were as follows: Cu 17.43%, In 13.38%, Ga 9.47%, Se 42.85%, Zn 0.50%, Cd 3.12%, S 3.70%, and O 9.58%. When the ZnS deposition time increased from 5 min to 10 and 15 min, we observed ZnS gradually covering CdS, resulting in a lower Cd/(S+O) atomic ratio. When the ZnS deposition time was increased to 15 min, the atomic ratios became the following: Cu 16.80%, In 13.23%, Ga 9.70%, Se 43.59%, Zn 0.51%, Cd 2.48%, S 3.09%, and O 10.60%. The standard process for CdS thin films (as used to produce Control 1) takes 15 min for deposition and had the atomic ratio composition of Cd 7.24%, S 8.43%, and O 12.37%. As to the ZnS/CdS double-layer, the Cd atomic ratio on the surface of the film decreased with an increase of ZnS deposition time. It is clear that all the atomic ratios of Zn/(S+O) (listed as Table 2) are far less than that of Cd. This observation and Fig. 3 verify that the growth rate of the newly designed ZnS film is much slower in depositing CdS/ZnS film.

One main objective of this study was to explore whether the ZnS/CdS double-layer structure could replace the i-ZnO layer. The J–V

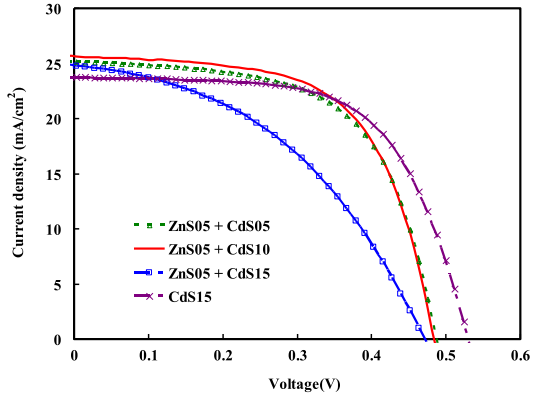

(*a*)

Samples No.	J_{SC} [mA/cm^2]	V_{OC} [V]	F.F. [%]	η [%]	R_S [Ω·cm^2]	R_{SH} [Ω·cm^2]
A1,CdS05+ZnS05	25.59	0.533	56.07	7.65	8.9	458
A2,CdS05+ZnS10	25.69	0.516	66.00	8.74	5.0	760
A3,CdS05+ZnS15	25.11	0.524	54.17	7.12	9.1	588
Ref 2, CdS15	24.61	0.531	62.40	8.15	11.1	1615

(*b*)

Fig. 5. (a) The J–V curves of CIGS solar cells made from different types of buffers with the ZnS /CdS structure, where the deposition time in the CBD bath has been varied as shown in Table 1. These structures were fabricated together with an i-ZnO layer. (b) Cell performance of CIGS solar cells with both the ZnS/CdS double-layer structure and the i-ZnO layer.

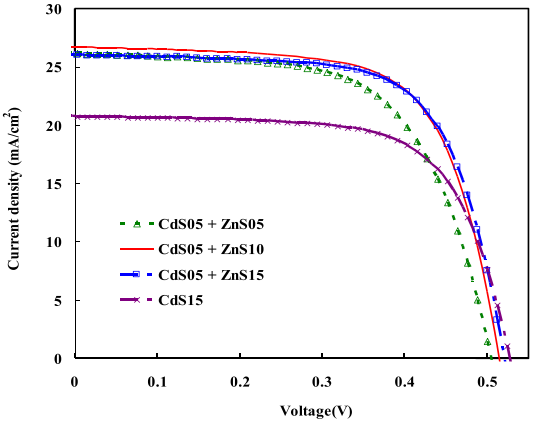

(*a*)

Samples No.	J_{SC} [mA/cm^2]	V_{OC} [V]	F.F. [%]	η [%]	R_S [Ω·cm^2]	R_{SH} [Ω·cm^2]
B1,CdS05+ZnS05	26.15	0.504	62.61	8.26	6.3	814
B2,CdS05+ZnS10	**26.72**	**0.515**	**67.16**	**9.23**	**4.9**	**899**
B3,CdS05+ZnS15	26.02	0.520	68.02	9.21	5.4	1238
Ref 1, CdS15	20.74	0.527	67.49	7.38	6.5	1440

(*b*)

Fig. 6. (a) The J–V curves of CIGS solar cells made from different types of buffers with ZnS /CdS structure, where the deposition time in the CBD bath has been varied as shown in Table 1. This structure was fabricated without an i-ZnO layer. (b) Cell Performance of CIGS solar cells with ZnS/CdS double-layer structure but without the i-ZnO layer.

curves and the performances of our CIGS solar cells with an i-ZnO layer are illustrated in Fig. 5. The curves and performances of these cells without an i-ZnO layer are shown in Fig. 6. The deposition times of A1/B1, A2/B2, A3/B3, and Control 2/ Control 1 in the CBD bath are the same as those listed in Figs. 3(b) and 4(b).

For the structures with an i-ZnO layer (Fig. 5b), the best sample is CdS 05+ZnS 10 with a ZnS/CdS double-layer buffer (sample A2). This sample yielded η of 8.74%, J_{SC} of 25.69 mA/cm^2, F.F. of 66.00%, and R_S of 5.0 Ω cm^2. When i-ZnO was added, the J_{SC} value of the Control 2 cell became 24.61 mA/cm^2, which was lower than the J_{SC} values for all the ZnS/CdS double-layer films (samples A1, A2 and A3). For the 10-min ZnS deposition, the comparisons between the J_{SC} and η of the ZnS/CdS structure and our previously studied CdS/ZnS structure (performance not shown here) showed that J_{SC} increased from 25.62 mA/cm^2 to 25.69 mA/cm^2 and η improved from 7.63–8.74%. The wider band gap of ZnS allows more incident high-energy photons to reach the buffer-absorber junction, which in terms increases J_{SC} (Fig. 5(b)) [15]. This is one of the main advantages of having ZnS deposited through CBD, as mentioned in [4] above.

Fig. 6 provides the CIGS-cell performances of the ZnS/CdS buffer and Control 1 without an i-ZnO layer; the J_{SC} of the Control 1 cell dropped to 20.74 mA/cm^2. Compared to the J_{SC} of the Control 2 cell with an i-ZnO layer (Fig. 5(b)), J_{SC} for Control 1 without an i-ZnO layer was 3.87 mA/cm^2 lower, and cell efficiency also decreased from 8.15–7.38%. For CIGS solar cells, the increase in J_{SC} could be attributed to a decrease in surface reflection [16]. When the shunt leakage of CIGS is sufficiently high, it can reduce the fill factor significantly while keeping J_{SC} and V_{OC} constant, which in turns adversely affects the cell efficiency [17]; therefore, a decrease in J_{SC} for Control 1 is independent of the shunt leakage.

Fig. 6(b) shows that sample B2 (10-min ZnS deposition) yielded the highest efficiency of the ZnS/CdS buffer films, with J_{SC}=26.72 mA/cm^2, V_{OC}=0.515 V, R_S=4.9 Ω cm^2, and η=9.23%. However, according to Fig. 6(b), J_{SC} for all the ZnS/CdS buffer films (B1, B2, and B3 cells) are higher than that of Control 1, demonstrating that partial replacement of the CdS film by a ZnS film will effectively improve the J_{SC} while also satisfying the environmental requirement for Cd-usage reduction. The double-layer buffer structure designed in this work can form a good Zns/CdS/CIGS heterojunction [18] and improve the transmittance in the short-wavelength region as described in Fig. 4. In addition, CBD-CdS/CIGS has better band alignment than CBD-ZnS/CIGS [19,20], further indicating that the efficiency of the CIGS cell can be improved. A performance gain was achieved by alloying the ZnS with CdS to widen the band gap [21]. In comparison, the performance of the B2 cell (CdS05+ZnS10 at Fig. 6) without an i-ZnO layer is better than that of the A2 cell (CdS05+ZnS10 at Fig. 5) with an i-ZnO layer. This shows that the i-ZnO layer does not improve performance.

Fig. 7 shows the external quantum efficiency (EQE) for our CIGS cells with three kinds of buffers: B2 (ZnS/CdS double-layer with i-ZnO/AZO), A2 (ZnS/CdS double-layer with AZO) and Control 2 (CdS buffer layer only). A significantly enhanced blue response of the cell with the ZnS/CdS buffer was observed, in concurrence with literature reports [22]. For the EQE of the MgF_2/ZnO/CdS/CGIS solar cell, the blue response was constrained by the band gaps of ZnO and CdS, and the red response was constrained by the band gap of the absorber [11]. In

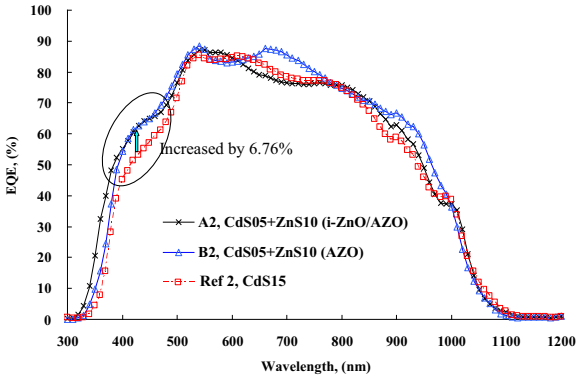

Fig. 7. The EQE of CIGS cells with double-layer buffer ZnS/CdS, compared to that of the control cell. The EQE of the CIGS solar cells with the ZnS/CdS buffer layer is about 6.8% higher than that of the Control 2 cell.

this study, for the short-wavelength range (350–500 nm), the average EQE value of our ZnS/CdS buffer structure was greater than that of the Control 2 cell by 6.8%, due to the high transmittance of the buffer layer [23]. This was attributed to the light absorption effect [24]—the buffer structure (ZnS/CdS double layer) adopts wider bandgap of ZnS (3.25 eV), thus allowing more incident light into the main absorption layer. Meanwhile, this double-layer thickness was about 31–42 nm (Fig. 3(b)), which was close to one-fourth of the wavelength (λ=410.61 nm) for the refractive index (n=2.551); therefore, the ZnS/CdS buffer could increase the fraction of incident light reaching the main absorption layer. The improvement of EQE is also consistent with the increase of values of J_{SC} as shown in Fig. 5(b) and in Fig. 6(b). Even if bandgap of CdS film is 2.4 eV, in general, the transmittance increases with the film thickness. As a result, the ZnS/CdS film shows higher transmittance compared to single CdS film, thus increasing the Jsc value and agreeing with the curves in Fig. 4(a).

4. Conclusions

In CIGS solar cells, thin-film depositions must be done in accordance with the tuneable band-gap values and in the following order starting from the top layer: 3.29 eV for the window layer (AZO), 3.25 eV for the ZnS buffer layer cubic form and 2.4 eV for the CdS buffer layer in cubic form, and finally 1.2 eV for the absorption layer (CIGS). This approach enables most of the incident light to enter the main absorption layer of the CIGS solar cells. An increase in visible light transmittance for ZnS/CdS-buffer cells (Fig. 4) enhances electrical performance, provided there is no loss from the photo-harvesting approach. This is verified by the J–V measurement of the cells, illustrated in Figs. 6 and 7.

For the ZnS/CdS buffer structure without an i-ZnO layer, the values for J_{SC} for sample B2 and η increased by 26.72 mA/cm^2 and 9.23%, respectively. In the meantime, we observe that with the substitution of ZnS/CdS for CdS single-layer buffers, the values of light transmittance and EQE in the short-wavelength region (300–500 nm) can be effectively improved, and the heterojunction can maintain good AR characteristics, thus enhancing cell performance. The experimental results demonstrate that the ZnS/CdS double-layer structure can omit the i-ZnO layer and still maintain good electrical and opto-electronic properties. Furthermore, this improvement can be achieved while reducing the usage of Cd, an undesirable material that could cause environmental hazard. The discoveries of this CIGS research provide a new scientific understanding of solar cells. In conclusion, this research undeniably contributes to a major advancement towards practical PV applications and can help building a more eco-friendly community.

Acknowledgment

The authors acknowledge the assistance and partial financial support of Ministry of Science and Technology (MOST 105-2221-E-019-067), and Chang Gung Memorial Hospital (CMRPG 2F0211) of Taiwan, respectively.

References

[1] M. Reinhard, C. Simon, J. Kuhn, L. Bürkert, M. Cemernjak, B. Dimmler, U. Lemmer, A. Colsmann, Cadmium-free copper indium gallium diselenide hybrid solar cells comprising a 2-(4-biphenylyl)-5-(4-*tert*-butylphenyl)-1,3,4-oxadiazole buffer layer, Appl. Phys. Lett. 102 (063304) (2013) 1–4.

[2] M.A. Islam, Y. Sulaiman, N. Amin, A comparative study of BSF layers for ultra-thin CdS: o/cdte solar cells, Chalcogenide Lett. 8 (2) (2011) 65–75 (Feb.y).

[3] P.K. Nair, M.T.S. Nair, V.M. Garcia, O.L. Arenas, Y. Pena, A. Castello, I.T. Ayala, O. Gomezdaza, A. Sanchez, J. Campos, H. Hu, R. Suarez, M.E. Rincon, Semiconductor thin films by chemical bath deposition for solar energy related applications, Sol. Energy Mater. Sol. Cells 52 (1998) 313–344.

[4] T. Nakada, K. Furumi, A. Kunioka, High-effciency cadmium-free Cu(In,Ga)Se2 thin-film solar cells with chemically deposited ZnS buffer layers, IEEE Trans. Electron Devices 46 (10) (1999) 2093–2097.

[5] C.Chien, C.Chen, C.Tsai, J.Shieh, Y.Hsiao, C.Lai, Performance improvement of CIGS solar cells with CBD-ZnS buffer layers by light soaking and rapid thermal annealing, in: Proceedings of the 37th IEEE Photovoltaic Spec. Conference (PVSC), Seattle, WA, USA, Jan, 2011, pp. 1255–1258.

[6] M.A.Contreras, T.Nakada, M.Hongo, A.O.Pudov, J.R.Sites, ZnO/ZnS(O,OH)/Cu(In,Ga)Se_2/Mo solar cell with 18. in: 6% efficiency, in Proceedings of the 3rd World Conference on Photovoltaic Energy Conversion, Osakapp, Japan, 11-18 May, 2LN-C-08, 2003, pp. 570–573.

[7] L. Zhou, Y. Xue, J. Li, Study on ZnS thin films prepared by chemical bath deposition, J. Environ. Sci. 21 (2009) S76–S79.

[8] A. Goudarzi, G.M. Aval, R. Sahraei, H. Ahmadpoor, Ammonia-free chemical bath deposition of nanocrystalline ZnS thin film buffer layer for solar cells, Thin Solid Films 516 (2008) 4953–4957.

[9] S.D. Sartale, B.R. Sankapal, M. Lux-Steiner, A. Ennaoui, Preparation of nanocrystalline ZnS by a new chemical bath deposition route, Thin Solid Films 480–481 (2005) 168–172.

[10] Rong-Fuh Louh, Warren Wu, Zinc sulfide nanoscaled buffer layers for Cu(In,Ga)Se_2 thin film solar cells by chemical bath deposition, Adv. Mater. Res. 51 (2008) 125–130.

[11] F. Ouachtari, A. Rmili, S.E. Bachir Elidrissi, A. Bouaoud, H. Erguig, P. Elies, Influence of bath temperature, deposition time and [S]/[Cd] ratio on the structure, surface morphology, chemical composition and optical properties of CdS thin films elaborated by chemical bath deposition, J. Mod. Phys. 2 (2011) 1073–1082.

[12] B. Elidrissi, M. Addou, M. Regragui, A. Bougrine, A. Kachouane, J.C. Bernède, Structure, composition and optical properties of ZnS thin films prepared by spray pyrolysis, Mater. Chem. Phys. 68 (2001) 175–179.

[13] Dong Hyeop Shin, Liudmila Larina, Kyung Hoon Yoon, Byung Tae Ahn, Fabrication of Cu(In,Ga)Se2 solar cell with ZnS/CdS double layer as an alternative buffer, Curr. Appl. Phys. 10 (2010) S142–S145.

[14] R.Mickelsen, W.S. in: Chen, Polycrystalline thin film CuInSe2 solar cells, in: Proceedings of the 16th IEEE Photovoltaic Specialist Conference, San Diego, CA, Sep. 27–30, 1982, pp. 781–785.

[15] M.A.Islam, M.S.Hossain, M.M.Aliyu, Y.Sulaiman, M.R.Karim, K.Sopian, N. in: Amin, Comparative study of ZnS thin films grown by chemical bath deposition and magnetron sputtering, in: Proceedings of the 7th International Conference on Electrical and Computer Engineering, Dhaka, Bangladesh, Dec, 2012, pp. 86–89.

[16] T. Kobayashi, K. Yamauchi, T. Nakada, Comparison of cell performance of ZnS(O,OH)/CIGS solar cells with UV-assisted MOCVD-ZnO: b and sputter-deposited ZnO:Al window layers, IEEE J. Photovolt. 3 (3) (2013) 1079–1083.

[17] S. Dongaonkar, J.D. Servaites, G.M. Ford, S. Loser, J. Moore, R.M. Gelfand, H. Mohseni, H.W. Hillhouse, R. Agrawal, M.A. Ratner, T.J. Marks, M.S. Lundstrom, M.A. Alam, Universality of non-Ohmic shunt leakage in thin-film solar cells,, J. Appl. Phys. 108 (124509) (2010).

[18] A. Luque, S. Hegedus, Handbook of Photovoltaic Science and Engineering, John Wiley & Sons Ltd, West Sussex, England, 2003, p. 585.

[19] A. Pudov, J. Sites, T. Nakada, Performance and loss analyses of high-efficiency chemical bath deposition (CBD)-ZnS-Cu($In_{1-x}Ga_x$)Se_2 thin-film solar cells, Jnp. J. Appl. Phys. 41 (2002) L672–L674.

[20] M. Morkel, L. Weinhardt, B. Lomuller, C. Heske, E. Umbach, W. Riedl, S. Zweigart, F. Karg, Flat conduction-band alignment at the CdS/$CuInSe_2$ thin-film solar-cell heterojunction, Appl. Phys. Lett. 79 (2001) 4482–4484.

[21] M. Estela Calixto, M.L. Albor-Aguilera, M. Tufino-Velazquez, G. Contreras-Puente, A. Morales-Acevedo, Ch.11 of Solar Cells–Thin-Film Technologies, InTech, Rijeka, Croatia, 2011 (ISBN: 978-953-307-570-9).

[22] K.Aryal, Y.Erkaya, G.Rajan, T.Ashrafee, A.Rockett, R.W.Collins, S.Marsillac, Comparative Study of ZnS thin films deposited by CBD and ALD as a buffer layer for CIGS cell, in: Proceedings of IEEE 39th Photovoltaic Spec. *Conference* (PVSC), Tampa Bay, Florida, USA, Jun, 2013, pp. 1101–1104.

[23] L.Larina, K.Kim, K.Yoon, M.Konagai, B.Ahn, Thin film CIGS-based solar cells with an In-based buffer layer fabricated by chemical bath deposition, in: Proceedings of the 3rd World Conference on PV Energy Conversion, vol. 1, Osaka, Japan, 2003, pp. 531–534.

[24] B.G. Prevo, Y. Hwang, O.D. Velev, Convective assembly of antireflective silica coatings with controlled thickness and refractive index, Chem. Mater. 17 (2005) 3642–3651.